**ROYAL
AERONAUTICAL
SOCIETY**

RESEARCH ARTICLE

Investigation on elastomer behaviour when exposed to conventional and sustainable aviation fuels

J. Hamilton[1] (ID), K. Elliott[2] (ID), P. Singh[3] (ID) and B. Khandelwal[1] (ID)

[1]Mechanical Engineering Department, The University of Alabama, Tuscaloosa, AL, USA
[2]Parker Aerospace, Fort Worth, TX, USA
[3]Department of Mechanical Engineering, National Institute of Technology Agartala, Agartala, Tripura, 799046, India
Corresponding author: B. Khandelwal; Email: bhupendra.khandelwal@gmail.com

Abstract

The aviation industry's efforts to reduce carbon emissions have driven the rapid development and scale-up of sustainable aviation fuels (SAFs). SAFs have the potential to significantly reduce CO_2 lifecycle emissions by up to 80% in comparison to Jet A and other conventional fossil-derived jet fuels. For multiple logistical and practical reasons, it is preferable to ensure that SAFs are 'essentially identical' (also referred to as 'drop-in SAF') to conventional jet fuel in terms of their performance, durability and compatibility with existing hardware systems. Because the majority of SAFs are not identical (non-drop-in) to conventional jet fuel, they have not been approved for use in their neat (100%) form. Instead, these non-identical SAFs are named synthetic blend components (SBC) as they are blended with conventional fuels to different extents per ASTM D7566-23a. It should be noted that there are on-going efforts to develop non-drop in SAF specifications to broaden their proliferation and maximise the aviation industries' ability to reduce CO_2 lifecycle emissions. One very important area of focus is the compatibility of SAFs with engine and fuel system seals, specifically understanding the dynamics of elastomeric seals. To address this, a novel approach has been developed to measure seal dynamics in flowing fuel. This technique has been applied to study the dynamic seal behaviour of four industrially relevant elastomer seals commonly employed in aviation fuel systems. The study involved three test fuels: (i) conventional fossil-derived Jet A, neat hydroprocessed esters and fatty acids (HEFA) SAF, and neat alcohol to jet (ATJ) SAF. Notably, both HEFA and ATJ fuels contain 0% aromatics, in contrast to Jet A, which typically contains around 17% aromatics by volume. The novel fuel-elastomer test rig used in this study was designed to simulate a practical scenario in which fuel flows through the inner surface of a pre-loaded static O-ring. The results of these tests demonstrate that the behaviour of different nitrile elastomers is unique to their formulation, and in all cases, the behaviour in HEFA and ATJ SAF differs significantly from that in Jet A. However, new fuel approval tests may only list one type of elastomer for evaluation, for example the 'Fit-for-Purpose' test in ASTM D4054-22 Tier 2 lists one specific nitrile. The findings of this study highlight the complexities of fuel-elastomer interactions within nominally identical chemical families and emphasise the potential risks of assessing compatibility based on tests conducted with a single member of a chemical family.

Nomenclature

AJF	alternative jet fuels
FT	Fischer–Tropsch
F_n/F_i	incremental force/initial force
FKM	fluorine kautschuk material (fluorocarbon-based elastomer)
FS	full scale

FVMQ	fluorosilicone
HEFA	hydroprocessed esters and fatty acids
IRHD	international rubber hardness degrees, microhardness testing
M_1	initial mass
M_2	mass after test
NBR	acrylonitrile butadiene copolymer, also referred to as nitrile
PNA	polynuclear aromatics
SAF	sustainable aviation fuel
SBC	synthetic blend component

1.0 Introduction

Sustainable aviation fuels (SAFs), also referred to as alternative jet fuels (AJF), are defined by The International Air Transport Association (IATA) as meeting certain sustainability criteria, including life-cycle carbon emission reduction, a limited fresh-water requirement, no competition with food production (in contrast to first-generation biofuels) and no deforestation. Carbon emission reduction is a global industrial goal and SAFs have the potential to reduce CO_2 lifecycle emissions by up to 80% [1]. Unlike conventional jet fuels, which are refined from crude oil feedstock, SAFs are produced from various sources, such as sugars, wood, agricultural oils or residues, municipal waste/waste gases, or cooking oil and/or through alternative synthetic processes that employ renewable energy [2–4]. Examples of SAFs include certain sustainably produced synthetic paraffinic kerosene (SPK) fuels, such as alcohol to jet (ATJ) and hydroprocessed esters and fatty acids (HEFA). Fuels produced through the Fischer-Tropsch (FT) process may also be considered SAFs, if they are produced using green hydrogen [5].

It is estimated that SAFs will be the dominant contributor to the reduction of aviation related CO_2 emissions by 2040 [6]. Along with the well-documented CO_2 emission reduction potential, SAFs typically bear lower aromatic and sulfur content, which reduces the particulate matter (PM) and sulfur dioxide (SO_2) emissions as compared to conventional fuel. To date, SAF PM emissions have been measured at 4x lower than conventional fuel [7,8]. Currently, there are multiple SAFs in production, each with unique feedstocks and production processes. For a SAF to be safely employed in aviation equipment, a complete understanding of the interactions between a SAF and the fuel-wetted aircraft components is essential [9].

As of this writing, no SAF has received regulatory approval to be used in its pure form (100%). To maintain Jet A-like properties, SAFs are only approved when blended to varying extents with conventional jet fuel. The blend ratio depends upon the specific SAF used and the resulting aromatic content of the blended fuel. ASTM D7566-21 compliant blending produces a fuel that can serve as a fungible replacement for Jet A. The current maximum blend ratio, as per ASTM D7566-21, stands at 50% with a minimum aromatic content of 8% v/v [10] with other SAF blends capped at lower percentages. These blend ratios have been determined through extensive physical property and fit-for-purpose tests conducted upon each SAF in its neat and blended fuel form [11]. SAF candidates must meet the requirements based on the properties of jet reference fuel (JRF) specified in ASTM D4054-22, which is the standard practice for evaluation of new aviation turbine fuels and fuel additives. The relevant properties are listed in Table A3.1 of this standard [12].

Several studies have demonstrated that the chemical composition of fuels significantly influences the performance and compatibility of materials they interact with [10–12]. One critical area concerns elastomer selection in fuel systems [13]. O-rings are typically formulated using a range of organic polymers, such nitrile rubber, fluorosilicone, fluorocarbon, polyurethane or neoprene. Nitrile rubber is commonly referred to as acrylonitrile butadiene copolymer (NBR). Figure 1 illustrates the basic molecular structures of acrylonitrile and butadiene, while Fig. 2 shows NBR in a singular molecular structure.

The acrylonitrile content may vary from 18% to 50% in NBR O-rings and tuning it allows physical and chemical properties to be tailored to the end application [14,15]. Increasing the acrylonitrile content raises hardness and fuel resistance, but reduces its durability and low-temperature properties.
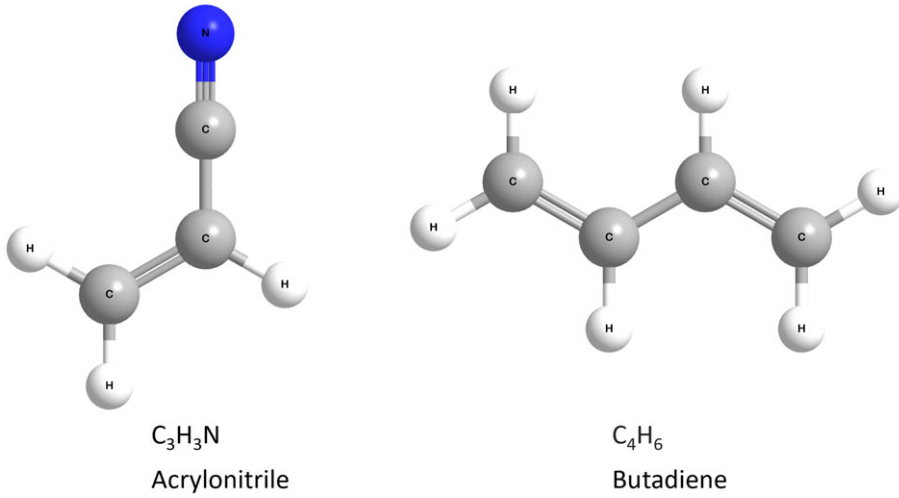
Acrylonitrile-Butadiene (NBR)

C_3H_3N

Acrylonitrile

C_4H_6

Butadiene

Figure 1. *Basic structures of the components of nitrile (NBR) rubber.*
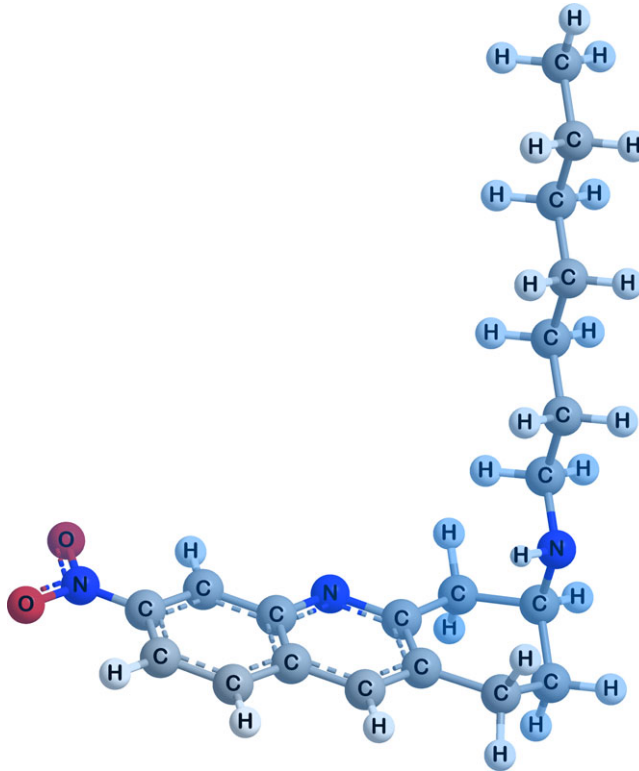
Figure 2. *Nitrile (acrylonitrile-butadiene) NBR polymer structure.*

C$_4$H$_7$F$_3$OSi

Fluorosilicone or Fluorovinylmethylsiloxane

(trifluoropropyl groups next to the methyl groups)
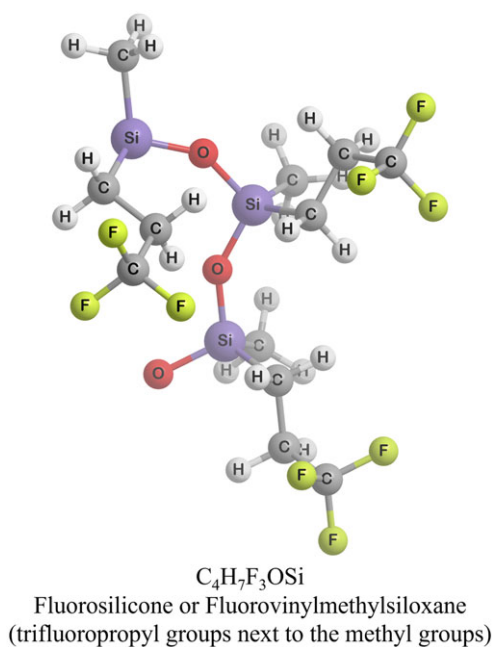
Figure 3. *Typical example of a fluorosilicone rubber structure. These molecules are composed of carbon, hydrogen, fluorine, oxygen and silicon.*

Linhares et al. concluded that an increase in the acrylonitrile content of NBR elastomers prevented their degradation in diesel fuel [16]. Nitrile O-rings exhibit resistance to various fuels and chemicals, although the level of resistance varies depending on factors such as the type of rubber, amount/type of filler, softener and vulcanising unit used [17]. However, despite their resistance to the specified factors in aviation applications, O-rings are still susceptible to different forms of stress, including thermal, mechanical and chemical stresses [18]. Chemical stress occurs when there is a change in the O-ring's molecular structure. The molecular structure forms a stranded network consisting of cross-linked and molecularly entangled strands [19]. The stiffness of the O-ring is directly related to these cross-linked chains, where a higher density of chains results in a stiffer elastomer. The stiffness value is typically determined through the shore A test process. Flory notes that an elastomer's ability to swell is a function of its elastic free energy, which is also influenced by the structures of the molecular chains in the elastomer [20].

Research has been conducted to better understand the chemistry of cross-linked chains and their effects on swell behaviour. For example, Jin et al. sought to improve elastomer mechanical properties by testing different blends of polyurethane elastomers [21]. It was observed that by adjusting the elastomer-curing parameter R value and ethylene oxide-co-tetrahydrofuran/polyethylene glycol ratio, elastomer swelling characteristics could be modified. Lower R values yielded the greatest elastomer swell, while increasing R decreased it.

Fluorosilicone (FVMQ) contains trifluoromethyl groups which terminate at each carbon chain (as shown in Fig. 3) and combines the impressive temperature properties of silicone, but improves upon its fuel and oil resistance. Fluorosilicones can generally operate over a significantly wider temperature range than fluorocarbon (FKM) elastomers. The use of fluorosilicone elastomers for aerospace applications has increased in recent years despite their higher cost over nitriles. Table 1 depicts a qualitative comparison of fluorosilicone and nitrile polymer properties.

In addition to aromatics, jet fuel contains other chemical families, such as n-paraffins (straight chain), i-alkanes (branched chain alkanes), naphthenes (cycloalkanes) and olefins (alkenes). Zabarnick et al. employed ASTM analytical protocols to characterise jet fuel composition [22]. The study concluded that petroleum jet fuels typically contain 80–85% paraffinic hydrocarbons and 15–20% aromatics, with

Table 1. *Comparison of fluorosilicone and nitrile polymers with selected properties [14]*

Elastomer Type (Polymer)	Abrasion Resistance	Chemical Resistance	Cold Resistance	Dynamic Properties	Heat Resistance	Impermeability	Set Resistance	Tear Resistance	Tensile Strength
Fluorosilicone	P	E	GE	P	E	P	G	P	F
Nitrile	G	FG	G	GE	G	G	GE	FG	GE

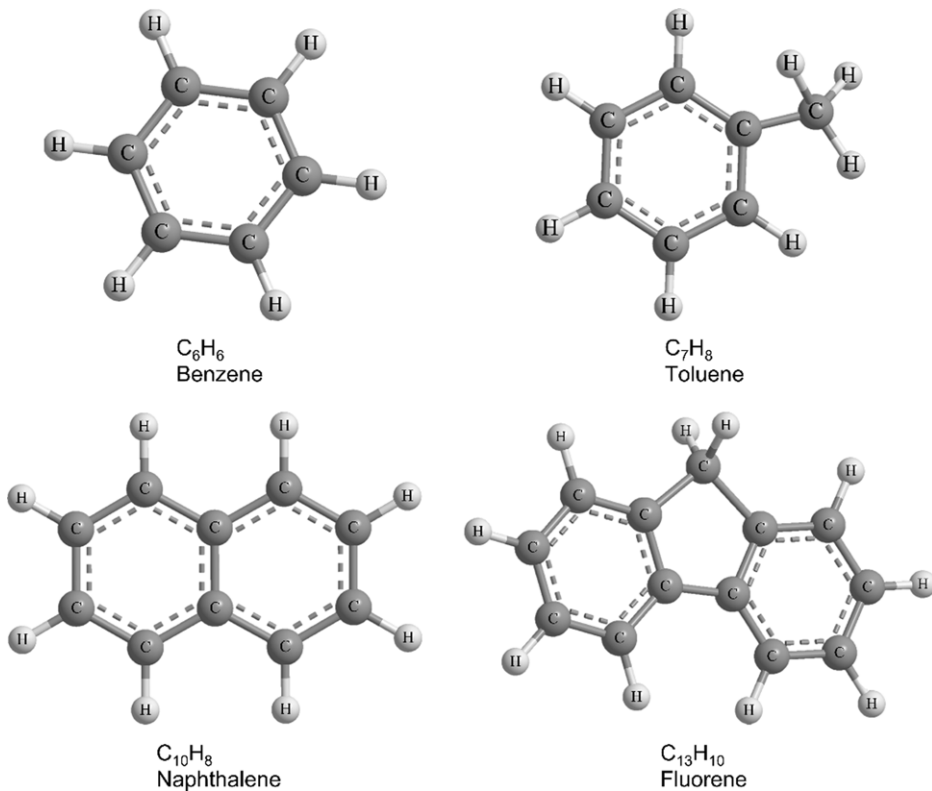P = Poor   F = Fair   G = Good   E = Excellent

Figure 4. *Examples of aromatic structures, naphthalene and fluorene are polynuclear aromatics (PNA) and have fused ring structures.*

very small fractions of the other components. Aromatic structures promote seal swell to facilitate leak-tight connections, however, the incomplete combustion of aromatics generates soot, known as particulate matter (PM), which is undesirable [23]. The aromatic content is a specification-controlled parameter in Jet A, as per ASTM D1655−22a, where it is limited to 25% by volume, when measured in accordance with ASTM D1319-20a [24]. Aromatic structures are often substituted derivatives of benzene, though fused ring structures, known as polynuclear aromatics (PNA) also exist [25]. Figure 4 provides several examples of aromatic structures, which have been detected in jet fuel. The majority of 100% SAFs, including the HEFA and ATJ fuel detailed herein, have negligible aromatic content [26]. In contrast, conventional jet fuels typically contain around 17% v/v aromatics [27].

Chen et al. provided practical evidence of the vital role aromatics play in achieving effective seal swelling [28]. They documented reports from commercial airlines that experienced fuel tank leakages. The root cause of these leaks was attributed to inadvertent refueling of the aircraft with low aromatic content (<8%) fuel. In some instances, the aromatic content of the fuel was only 1.4% v/v. In 2009, NASA conducted experiments on a test aircraft fueled with a 100% Fischer-Tropsch processed fuel, which had 0% aromatics. These experiments resulted in fuel leaks, which lead to the pooling of fuel under the aircraft. To address the issue, the aircraft fuel tanks were drained and refueled with Fischer-Tropsch fuel containing 9.7% aromatics by volume [29].

When an O-ring swells or shrinks, a change in volume of the seal occurs, which may cause changes in other physical properties such as compression set, hardness and tensile characteristics [19]. These property changes influence the effectiveness of the seal between connected fuel components. Some research has focused on establishing a more comprehensive understanding of fuel-elastomer interactions. Anuar et al. concluded that the relationship between aromatic structures and seal swelling is linear [30]. However, Graham et al. studied the swelling of nitrile rubber by doping synthetic fuel with a range of aromatics and concluded that fuel-elastomer interactions are highly complex and depended upon the partition coefficient [31].

The partition coefficient also provides a measure of fuel-elastomer interaction [32]. Nitrile elastomer swelling behaviour was found to increase with the increase in polarity and hydrogen bonding character of the aromatics [33]. This suggests that the swelling of nitrile rubber is facilitated by the disruption of attractive forces between cyano groups on adjacent polymer chains, where they are replaced with cyano-aromatic interactions. Additionally, volume swell was found to decrease with increasing molecular weight. As seal swell results from a complex interplay of intermolecular forces at the nanoscale, the chemical properties of both the fuel and the seal ultimately determine the macroscopic effect on the seal.

Corporan et al. described the fundamental fuel properties which impact elastomer swell which include molar volume, polarity and the ability of the fuel to provide hydrogen for hydrogen bond formation [34]. They also noted that SAFs have diminished ability to be an effective hydrogen donor as well as having low polarity. For these reasons, it is necessary that important physical properties of elastomers are identified, known and understood. Typically, elastomer compatibility tests include measurements of elastomer hardness, tensile strength, elongation, compression set and volume swell.

Despite the extensive volume of research on seal swell, it remains evident that the amount and rate of seal swell is highly dependent upon seal material. Adams et al. studied a range of elastomers in fuels of varying aromatic content, and those tests revealed that swell was proportional to the aromatic content [35]. Findings were corroborated by Luning et al. [36].

A review of published studies on elastomer compatibility with aviation fuels highlights certain knowledge gaps which must be addressed. Standardisation for testing the complex interactions between O-rings and different fuels is available in various ASTM documents. These standards define test methods and equipment used by researchers to validate their data. However, some elastomer test methods are outdated and may not represent on-wing applications. Furthermore, knowledge gaps may also arise since ASTM standards call for the selection of single O-rings from each chemical family. An assumption is made that results obtained on the selected O-ring are representative of the entire polymer group, and this may not necessarily be valid. For example, ASTM D4054-22 Tier 2 testing is conducted using a single O-ring selected from three disparate polymer families, as summarised in Table 2. It may not be the intention of the standard to require the exact O-rings listed to be tested, but in practice this is how the standard is generally interpreted. For instance, an FAA partition coefficient test programme only tested the O-rings from Table 2 and the results may not be applicable to other O-rings considered to be the same 'kind' [37].

The present study was designed to address some of these knowledge gaps and expand research data on the topic. The aim of this study is to investigate the reactions of elastomers with Jet A and SAF fuels and to identify potential diversity in the behaviour of nitrile elastomers. The experiments were conducted using a novel fuel-elastomer compatibility test rig, specifically designed to simulate the actual installation of O-rings in fuel systems. The validity of the apparatus and data was evaluated through

Table 2. *Elastomer O-ring seals listed in for D4054 Tier 2 fit-for-purpose compatibility properties testing*

Polymer type	Model number
Nitrile	N0602-70
Fluorosilicone	L1120-70
Fluorocarbon	V1226-75

Table 3. *Material properties listed in physical testing reports and IRHD microhardness tests (conducted by ARDL) for the 2-113 O-rings (13.94mm ID, 2.62mm CS)*

Part number	Polymer	Temperature range (°F)	Durometer A hardness (pts)	IRHD hardness (pts)	Tensile strength	Specific gravity (g/cm³)
LM100-70	Fluorosilicone (FVMQ)	−100–350	62	64	1,417	1.46
N0602-70	Low set nitrile (NBR)	−70–180	63	67	1,254	1.27
NM072-70		−60–180	65	68	1,799	1.31
N0674-70		−30–250	67	70	2,546	1.22

Table 4. *Aromatic content of the test fuels*

Fuel	Aromatic content (v/v %)*
Jet A	17
HEFA-SPK (SAF)	0.1
ATJ-SPK (SAF)	<0.001

*Determined by ASTM D6379

comparison to published data obtained using commercial test equipment. The test rig described herein provides more representative test conditions, extended test durations, and enabled real-time monitoring of elastomer internal forces. The decision to select several O-rings from the nitrile family was motivated by both the diversity in nitrile properties and to evaluate the level of risk associated with the selection of a single O-ring to represent an entire polymer family.

2.0 Methodology

2.1 Materials

The present study utilises dynamic elastomer tests with a focus on multiple aviation fuels and elastomer chemistries. Employing the equipment described herein, the study evaluated O-ring polymers of fluorosilicone and three types of low set nitrile against Jet A, HEFA SAF and ATJ SAF fuels. Table 3 summarises some of the nominal physical properties of the elastomer seals evaluated in this study.

2.2 Fuels

Three fuels were used in this study: Jet A (conventional jet fuel derived from crude oil), HEFA (hydroprocessed esters and fatty acids), and ATJ-SPK (alcohol-to-jet synthetic paraffinic kerosene). The aromatic contents of these fuels are summarised in Table 4.

HEFA fuel is produced through the hydroprocessing of triglycerides sourced from animal fats and plant oils. ATJ involves the dehydration, polymerisation and hydrogenation of a short-chain alcohol. The basic production processes for HEFA and ATJ fuels are illustrated in Fig. 5.
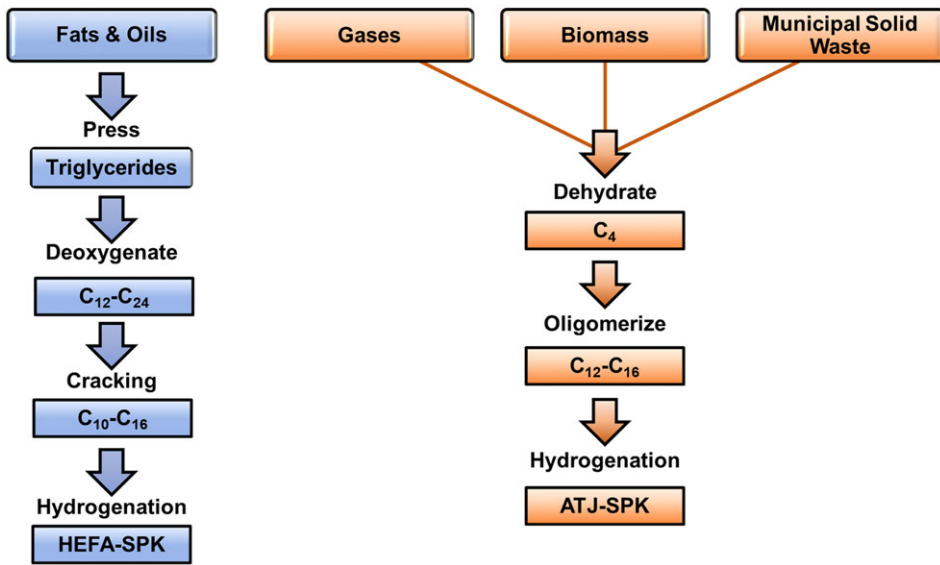
Figure 5. *HEFA-SPK (left) and ATJ-SPK (right) production processes.*

While HEFA and ATJ are currently approved for use when blended with Jet A, the ultimate goal of the industry is to maximise CO_2 lifecycle reduction potential through employment of SAFs without any Jet A blending. To mimic this scenario and to maximise experimental resolution, these SAFs will be employed in their unblended state in tests herein.

2.3 Experimental setup

Figure 6 illustrates the general schematic of the fuel-elastomer compatibility test rig. The rig is designed to measure the dynamic changes of elastomer seal internal forces while replicating a realistic installation environment. The rig applies an initial force to the O-ring to simulate the coupling of two components retained under the application of a specific torque. Throughout the experiment, this force is continuously recorded for later analysis. For each O-ring, an initial compression force of approximately ~3.6kgf (~35.3N) was applied. Because the seals are closely related in terms of hardness properties, the experiment was structured to maintain a constant compressive force rather than a fixed initial O-ring compression percentage value. Measurements of the internal forces were recorded at a frequency of 1Hz.

The components of the rig are made of stainless steel and molded plastic. All fuel-wetted parts are machined from stainless steel. A fuel pump maintains a constant flow of fuel though the internal surface of the O-ring. The pump, equipped with several vibration absorbers, is attached to the fuel reservoir/tank. The seal under test is seated between two stainless steel plates within precisely milled recesses in each plate. For data and trend analysis, each second of incremental force data observed (F_n) was averaged and then normalised against the initial compression force (F_i) according to Equation (1). The normalised value was further adjusted to indicate the change of internal forces as a percentage from the initial force, which serves as the characteristic dimension proportional to the swelling/shrinkage. All results are presented as plots of normalised percent swell/shrink vs time.

$$\text{Swell } \% = \ ((F_n/F_i) - 1) \cdot 100 \tag{1}$$

The experimental tests are conducted simultaneously using four identical test rigs. This approach ensures that data is collected under consistent external conditions. Throughout the tests, the ambient air temperature is maintained at 18°C ± 1°C. Each experimental run utilises the same type of fuel and
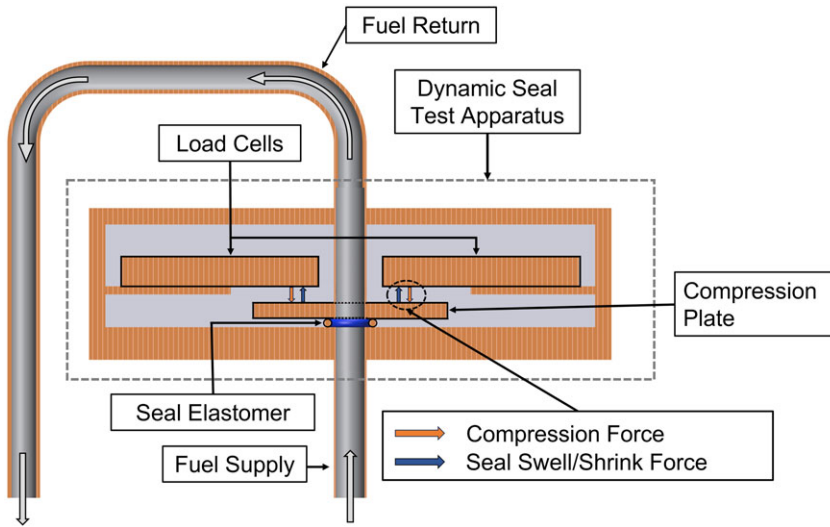
Figure 6. *General schematic of fuel-elastomer compatibility test rig system.*

with different O-rings installed in each rig. To ensure fidelity of the measurements the test rigs are equipped with separate fuel tanks, fuel pumps, AC/DC electrical systems and data acquisition modules. Despite these separate components, the fuel for each experimental run is sourced from the same supply to maintain uniformity in the testing process. When fuels are changed meticulous care has been taken to ensure cross contamination does not occur. This is accomplished through the application of protocols established by Vangsness [38] and in accordance with ASTD D4306-20 Standard Practice for Aviation Fuel Sample Containers for Tests Affected by Trace Contamination [39].

2.4 Measurement uncertainty

Measurements conducted using the elastomer dynamic compression system are not complex. O-ring swelling/shrinkage forces are directly measured by cantilever load cells placed directly in contact with a circular stainless-steel plate, which provides a structure for the forces to be applied to the O-ring emanating from set screws in the load cell. Each load cell is calibrated using a class 5 weight, and measurements are inputted directly into the load cell amplifier software. Load cells employ a full Wheatstone bridge electrical circuit and a thermocouple as a supplemental sensor.

Every effort has been made to reduce systematic measurement uncertainty effects. The primary function of the thermocouple is to monitor the temperature of the fuel approximately 5mm from the O-ring. The fuel temperature data is not used for any calculation of the O-ring reaction forces; thus, the uncertainty of the thermocouple is not required for the O-ring data, only to ensure that tests are conducted within an acceptable temperature range. The load cells use a full Wheatstone bridge where two of the four wires between the resistors are in compression and the others are in tension. This configuration is resistant to temperature changes with 0.003% Full Scale (FS)/°C. Documentation for the load cells used in the EDC system shows that the repeatability is 0.03% FS. The value of repeatability is very important as it limits the accuracy of the load cells. Equations (2)–(4) show the combined uncertainty (u_c) of the data at .09% FS. Sources of measurement error for the load cells used in this study are listed as follows:

- Corner load error $u_{cl} = 0.05\%$ FS
- Creep (per 5min) $u_{cr} = 0.05\%$ FS/3min
- Hysteresis $u_h = 0.03\%$ FS

- Non-linearity $u_{nl} = 0.03\%$ FS
- Repeatability $u_r = 0.03\%$ FS
- Temperature effect on sensitivity $u_{ts} = 0.003\%$ FS/°C
- Temperature effect on zero (per 10°C) $u_{tz} = 0.03\%$ FS/°C

$$u_c = \sqrt{u_{cl}^2 + u_{cr}^2 + u_h^2 + u_{nl}^2 + u_r^2 + u_{ts}^2 + u_{tz}^2} \tag{2}$$

$$u_c = \sqrt{.05^2 + .05^2 + .03^2 + .03^2 + .03^2 + .003^2 + .03^2} \tag{3}$$

$$u_c = .09\% FS \tag{4}$$

3.0 Results and discussion

The tests were conducted using identical experimental protocols over 100 hours. Beyond 100 hours of exposure in HEFA and ATJ fuel leaks were observed due to excessive O-ring shrinkage.

3.1 Effect of Jet A on elastomers

In the tests conducted with Jet A (Fig. 7), the results revealed a notable difference in the behaviour of nitrile O-rings compared to the fluorosilicone O-ring. While all nitrile O-rings initially experienced swelling when exposed to Jet A, the fluorosilicone O-ring exhibited shrinkage. This divergence in behaviour is likely attributed to the varying chemical compositions and molecular structures of the elastomers.

Furthermore, the swelling behaviour of the nitrile O-rings in Jet A showed distinct profiles, with different extents of swelling observed after 100 hours of exposure. Among the tested nitrile O-rings, N0602-70 exhibited significant swelling, with its volume increasing by approximately 26%. In contrast, NM072-70 displayed a much lower swell of around 5%, indicating a milder sensitivity to Jet A fuel. The N0674-70 swell behaviour at 100 hours reached approximately 12%. Interestingly, the three nitriles displayed unique swelling rates and magnitudes. The N0602-70 rate of swell was high for the first 20 hours then steadily decreased over time. The swell rate of N0674-70 was very steady until around 70 hours. The LM100-70 fluorosilicone behaviour consisted of a rapid initial shrinkage followed by a steady decrease characterised by some oscillatory behaviour. At the conclusion of the 100-hour test the LM100-70 had a value of -7% shrinkage.

These differences in the elastomer behaviours could be due to differences in the compositions of the elastomers, such as the proportions of acrylonitrile and butadiene in the nitrile O-rings. Since the exact chemistry employed in each elastomer is proprietary information, the authors have no insight into
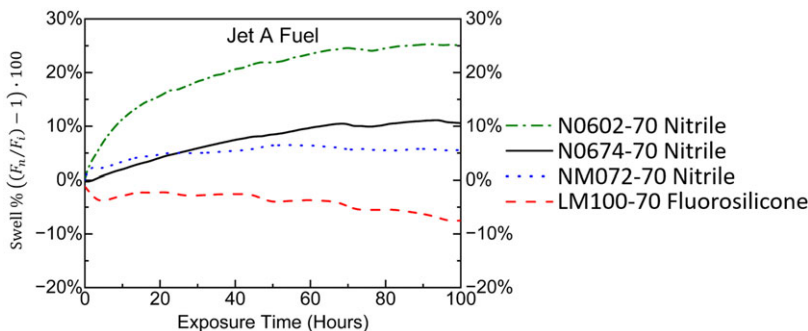

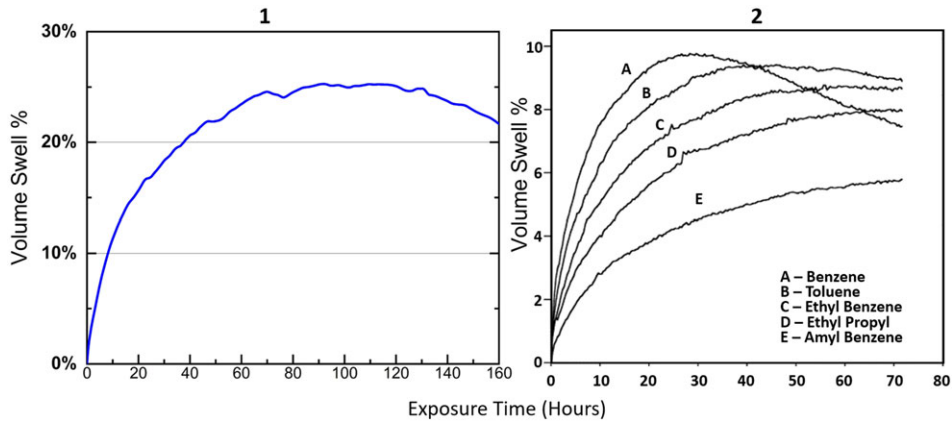**Figure 7.** *Results of seals compatibility tests with Jet A.*

Figure 8. *(a) N0602-70 reaction with Jet A from this study. (b) Data from Graham et al., N0602-70 nitrile reactions with different aromatics blended with synthetic JP-5. The blended fuels contained the same ratio of aromatics, 10% v/v [31].*

potential compositional differences. Previous research suggests that the acrylonitrile content significantly influences the elastomer's fuel resistance and swelling characteristics. The higher acrylonitrile content in nitrile rubber results in enhanced fuel resistance but may reduce low-temperature properties and resilience [40]. In addition to the formulation and acrylonitrile content, the behaviour of an elastomer can also be influenced by other factors, such as its molecular structure. These variations could explain the differences observed in the swelling behaviour of N0602-70 and NM072-70 over time.

These findings are consistent with previous studies that have shown that elastomers within the same chemical family can exhibit markedly different responses to fuel exposure due to variations in their polymer chain structure and cross-linking characteristics [31]. The disparity in the swelling behaviour between N0602-70 and NM072-70 is clear indication that not all nitrile O-rings are created equal, and behaviour obtained for one nitrile chemistry cannot be assumed to be the same for another.

The differential behaviour of nitriles is not only evident by the reaction of the nitrile elastomers during the Jet A tests, but also shown in the study from Graham et al. (shown in Fig. 8) where a single nitrile (N0602-70) was exposed to a range of substituted benzene aromatic components added to synthetic JP-5 fuel [31]. Note that the synthetic fuel and aromatic ratios were kept constant (10% v/v), only the aromatic identity was modified. As noted earlier, the benzene moiety is the most common aromatic structure in conventional jet fuel so there is an expectation that the swell observed in this study should bear broadly similar characteristics to that observed in our Jet A studies. Gratifyingly, results were in reasonable agreement.

Closer inspection showed that the Jet A reaction reached a maximum swell of ∼25% after 70 hours in our tests, while the benzene blend in Graham et al.'s study swell was ∼9% at 30 hours. These differences could be attributed to several factors. For instance, the aromatic content differed; in our study it was ∼17%, while Graham's was 10%. The aromatics in Jet A are not represented by a single component as they are in Graham's work. The experimental setups also utilised different methods for collecting volume swell data. The Jet A test was accomplished with compression and flowing fuel whereas the benzene blend data was recorded with the O-ring in a fuel bath and volume change was determined by optical dilatometry systems. JP-5 also differs from Jet A fuel.

3.2 Effect of HEFA on elastomers
Figure 9 shows the tests conducted with HEFA fuel, the three nitrile O-rings and the fluorosilicone O-ring. Overall, all O-rings exhibited very modest changes. This is likely due to the absence of aromatics
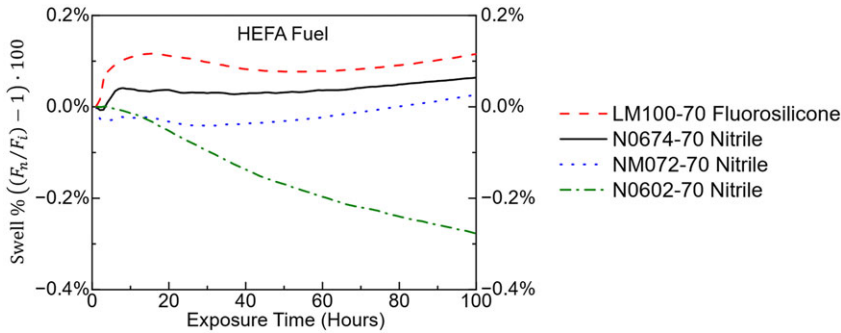
Figure 9. *Results of seals compatibility tests with HEFA.*

in HEFA fuel, unlike the Jet A ($\sim$17% v/v aromatics). Notably, the N0602-70 was the only O-ring to experience shrinkage, approximately -0.28% by 100 hours. The NM072-70 experienced very modest shrinkage during the first few minutes of the test followed by a slow but steady swell to approximately 0.03%. The LM100-70 and N0674-70 both experienced a sharp swell initially reaching a peak of 0.12% (at 14 hours) and 0.04% (at 7 hours), respectively. The N0674-70 showed very little reaction for the first 3 hours with a shrinkage of only -0.01% before the sharp increase in swell rate. The two O-rings then experienced a single phase of slight shrinkage then swell for the duration of the test. The final values for the two O-rings were 0.11% (LM100-70) and 0.06% (N0674-70).

Research conducted separately by Anuar and Chen has also highlighted the significant role of aromatic content in fuel in influencing the ability of O-rings to swell [30,41]. Their studies indicated that a higher aromatic content in the fuel contributes to enhancing the ability of O-rings to swell. Additionally, they found that the stress relaxation behaviour of O-rings is closely tied to the specific type of aromatics present in the fuel. These findings align well with the outcomes of our study. The absence of aromatics in HEFA may have a similar effect, causing shrinkage in the elastomers due to the reduced ability to promote seal swell. Moreover, the study by Faulhaber investigated the relationship between aromatic structures and seal swelling [42]. Faulhaber also found that elastomer swelling depends upon the presence of aromatics in the fuel and the chemistry of the elastomer.

3.3 Effect of ATJ-SPK on elastomers

In the evaluation of ATJ-SPK fuel, tested nitrile and fluorosilicone O-rings experienced shrinkage after 100 hours of exposure as seen in Fig. 10. Interestingly, the nitrile O-ring NM072-70 and fluorosilicone LM100-70 displayed opposing behaviour throughout the test but both reaching nearly the same shrinkage of -0.18% after 100 hours. The rate of shrinkage for the NM072-70 was much lower than the LM100-70 for the first 35 hours, with shrinkage of -0.04% and -0.19%, respectively. The N0602-70 behaviour was negligible showing only slight swell during the first two hours with a maxima of 0.06%. N0674-70 was most perturbed by ATJ with a value of -0.36% at the conclusion of the 100-hour test. In general, the O-rings demonstrated very little reaction with the ATJ-SPK fuel. Akin to HEFA fuel tests, the shrinkage observed in ATJ-SPK can also be attributed to the absence of aromatics in the fuel.

3.4 Results of Jet A, HEFA and ATJ-SPK with all tested O-rings

Figure 11 contains four graphs displaying the results of each individual O-ring and the reactions with the three fuels tested. Common *x*- and *y*-axis scales were employed for ease of comparison.

In the tests conducted with Jet A, the nitrile O-rings initially experienced swelling when exposed to the fuel. However, the extent of swelling varied depending on the type of nitrile O-ring. The N0602-70 O-ring exhibited the most swelling, with its volume increasing by approximately 26%. N0674-70 and
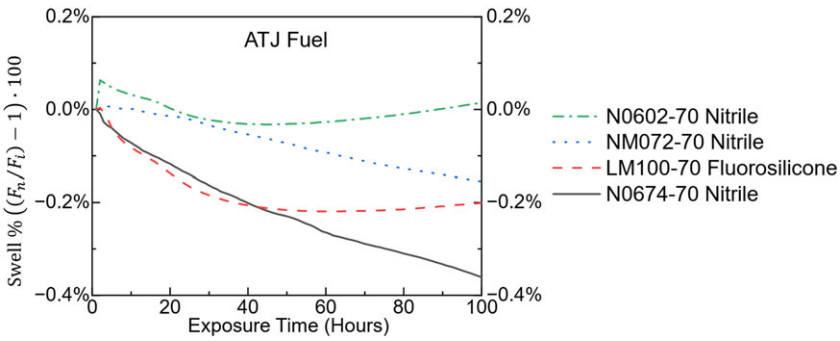
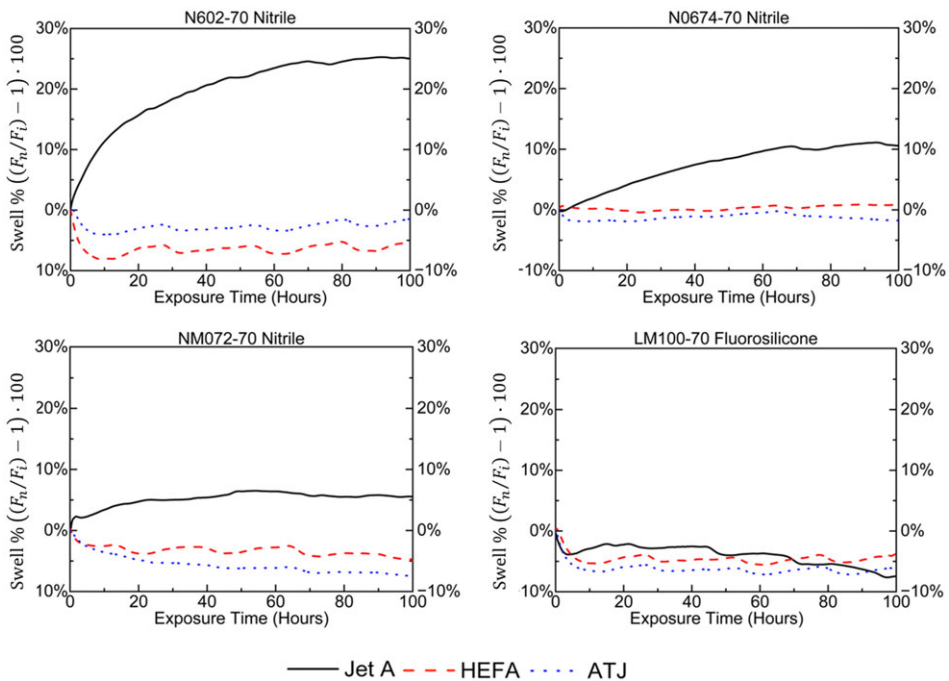**Figure 10.** *Results of the seals compatibility tests with ATJ-SPK.*

Figure 11. *Combined results of N0602-70 nitrile, N0674-70 nitrile, NM072-70 nitrile and LM100-70 flourosilicone with Jet A, HEFA, and ATJ-SPK fuels.*

NM072-70 O-rings experienced comparatively less swelling with Jet A fuel that is approximately 11% and 5%, respectively.

The fluorosilicone O-ring, LM100-70, exhibited the opposite behaviour. No positive swell was seen throughout the test. The overall trend for the LM100-70 was a relatively stable decline with fluctuations from -2.26 to -7.5%. This is likely due to the different chemical composition of fluorosilicone O-rings, which are not as susceptible to swelling as nitrile O-rings. The NM072-70 and the LM100-70 trends during the 100-hour test were similar as they remained relatively stable when compared to the N0602-70 and N0674-70 O-rings.

The tests conducted with HEFA and ATJ-SPK fuel showed that the nitrile and fluorosilicone O-rings shrink when exposed to the fuel. This is likely due to the absence of aromatics in these fuels. Aromatics

are present in conventional jet fuels like Jet A, and they play a crucial role in seal swelling and facilitate leak-tight connections. However, in the case of HEFA and ATJ-SPK, the fuel lacks these aromatic compounds, leading to a different interaction with the elastomers.

The radical departure of the N0674-70 O-ring from the trends observed in other seals highlights the diversity in nitrile behaviour. Each nitrile O-ring behaved in a unique manor depending on the fuel it was exposed to. Even within a common fuel, such as Jet A, significant variations in behaviour between the elastomers from the same nitrile chemical family were evident. This suggests that the chemical composition of the seal can influence the interactions of the polymer chains with aromatic compounds present in the fuel, subsequently affecting the internal force dynamics of the seal. Chen's research showed that material volume swell is not only affected by fuel properties, but also by the structure and properties of the material itself [41]. This finding is consistent with the results of the present study.

4.0 Conclusion

The observations from this study provide valuable baseline data on the reactions of elastomers with non-aromatic SAF fuels. This data contributes to a better understanding of the effects of different aromatic concentrations in future studies.

Some of the key conclusions are as follows:

- Nitrile behaviour is diverse; each nitrile O-ring behaves differently depending on the fuel it is exposed to, and significant differences exist in a common fuel, such as Jet A.
- The behaviour of one nitrile O-ring cannot be generalised to represent the behaviour of other nitriles.
- It is essential to evaluate multiple nitriles in fuel qualification programmes, which is currently a limitation in ASTM where only one nitrile is typically selected for testing.
- The three nitriles tested herein were found to swell in Jet A but tend to shrink in HEFA SAF and ATJ SAF, which lack aromatic content.
- Nitriles designed for use in Jet A applications, which rely on their ability to swell, are unsuitable for exposure to 100% HEFA or ATJ SAF because they shrink. This could lead to fuel leaks.
- Nitriles designed for use in Jet A applications cannot be used in switch-loading applications, where aircraft are fueled with Jet A at one airport and 100% SAF at another.
- In contrast, the LM100-70 fluorosilicone tested was found to exhibit low sensitivity to fuel type, whether it is Jet A or SAF, thus it holds promise for use in switch-loading applications.
- The LM100-70 fluorosilicone O-ring shrank in Jet A, HEFA and ATJ SAF to broadly comparable extents.
- Because the LM100-70 fluorosilicone behaviour in Jet A and SAF was similar, this O-ring can be used with 100% HEFA and 100% ATJ SAF, which lack aromatic content.

References

[1] The International Air Transportation Association. Net Zero 2050: Sustainable Aviation Fuels: Fact Sheet. Retrieved from https://www.iata.org/en/iata-repository/pressroom/fact-sheets/fact-sheet—alternative-fuels/

[2] Ling, C., Hamilton, J. and Khandelwal, B. Chapter 1 - Feedstock and pathways for alternative aviation fuels, in B. Khandelwal (Ed), *Aviation Fuels*, Academic Press, 2021, pp 1–22. https://doi.org/10.1016/B978-0-12-818314-4.00004-2

[3] Undavalli, V.K. and Khandelwal, B. Impact of alternative fuels and fuel properties on PM emissions, in *Aviation Fuels*, Elsevier, 2021, pp 71–111. https://doi.org/10.1016/B978-0-12-818314-4.00012-1

[4] Alternative Fuels Data Center U.S. Department Of Energy. Sustainable Aviation Fuel. 2023(06/26/2023). Retrieved from https://afdc.energy.gov/fuels/sustainable_aviation_fuel.html

[5] Kang, S. Effect of the accelerated aging on bio-jet fuel and contacted elastomer, *Polym. Bull.*, 2022, **79**, (1), pp 503–518. https://doi.org/10.1007/s00289-020-03526-4

[6] O'connell, A., Kousoulidou, M., Lonza, L. and Weindorf, W. Considerations on GHG emissions and energy balances of promising aviation biofuel pathways, *Renewable Sustainable Energy Rev.*, 2019, **101**, pp 504–515. https://doi.org/10.1016/j.rser.2018.11.033

[7] Landera, A., Bambha, R.P., Hao, N., Desai, S.P., Moore, C.M., Sutton, A.D. and George, A. Building structure-property relationships of cycloalkanes in support of their use in sustainable aviation fuels, *Front. Energy Res.*, **1010**, 2022. https://doi.org/10.3389/fenrg.2021.771697

[8] Pavlenko, N. and Searle, S. Fueling flight: Assessing the sustainability implications of alternative aviation fuels, The International Council on Clean Transportation, 2021. Retrieved from https://theicct.org/sites/default/files/publications/ https://theicct.org/sites/default/files/publications/

[9] Liu, Y. and Wilson, C.W. Investigation into the impact of n-decane, decalin, and isoparaffinic solvent on elastomeric sealing materials, *Adv. Mech. Eng.*, 2012, **4**, p 127430. https://doi.org/10.1155/2012/127430

[10] Kosir, S., Heyne, J. and Graham, J. A machine learning framework for drop-in volume swell characteristics of sustainable aviation fuel, *Fuel*, 2020, **274**, p 117832. https://doi.org/10.1016/j.fuel.2020.117832

[11] Undavalli, V., Olatunde, O.B.G., Boylu, R., Wei, C., Haeker, J., Hamilton, J. and Khandelwal, B. Recent advancements in sustainable aviation fuels, *Prog. Aerospace Sci.*, 2023, **136**, p 100876. https://doi.org/10.1016/j.paerosci.2022.100876

[12] ASTM Standard D4054-22. (2022). Standard Practice for Evaluation of New Aviation Turbine Fuels and Fuel Additives. https://doi.org/10.1520/D4054-22

[13] Druecke, B., Dussan, E.B.V., Wicks, N. and Hosoi, A.E. Large elastic deformation as a mechanism for soft seal leakage, *J. Appl. Phys.*, 2015, **117**, (10), 104511-104511-104511-104519. https://doi.org/10.1063/1.4914523

[14] Parker Seals. *Parker O-Ring Handbook (ORD 5700),* Parker Seal Group, 1992, Lexington, KY. Retrieved from https://www.parker.com/content/dam/Parker-com/Literature/O-Ring-Division-Literature/ORD-5700.pdf

[15] Mckeen, L.W. *Permeability Properties of Plastics and Elastomers*, William Andrew, 2016. https://doi.org/10.1016/C2010-0-66502-3

[16] Linhares, F.N., Corrêa, H.L., Khalil, C.N., Amorim Moreira Leite, M.C. and Guimarães Furtado, C.R. Study of the compatibility of nitrile rubber with Brazilian biodiesel, *Energy*, 2013, **49**, pp 102–106. https://doi.org/10.1016/j.energy.2012.10.040

[17] Białecki, T., Gawron, B., Giemza, B. and Głb, J. Influence of synthetic fuel on nitrile rubbers used in aviation, *Transport Problems*, 2020, **15**, (3), pp 29–41. https://doi.org/10.21307/tp-2020-031

[18] Lou, W., Zhang, W., Jin, T., Liu, X. and Dai, W. Synergistic effects of multiple environmental factors on degradation of hydrogenated nitrile rubber seals, *Polymers*, 2018, **10**, (8), p 897. https://doi.org/10.3390/polym10080897

[19] Qamar, S.Z., Akhtar, M., Pervez, T. and Al-Kharusi, M.S. Mechanical and structural behavior of a swelling elastomer under compressive loading, *Mater. Des.*, 2013, **45**, pp 487–496. https://doi.org/10.1016/j.matdes.2012.09.020

[20] Flory, P.J. Molecular theory of rubber elasticity, *Polym. J.*, 1985, **17**, (1), pp 1–12. https://doi.org/10.1016/0032-3861(79)90268-4

[21] Jin, P., Pang, A., Yang, R., Guo, X., He, J. and Zhai, J. Study on mechanical properties of polyurethane cross-linked P (E-co-T)/PEG blended polyether elastomer, *Polymers*, 2022, **14**, (24), p 5419. https://doi.org/10.3390/polym14245419

[22] Zabarnick, X., Phelps, D., West, Z., Shafer, L., Ervin, J., Dewitt, M., Binns, K., Williams, T., Dieterle, G., Balster, L. and E, H. (2008). Evaluation and Testing of the Suitability of a Coal-Based Jet Fuel, 72. Retrieved from https://apps.dtic.mil/sti/pdfs/ADA502844.pdf

[23] Bernabei, M., Reda, R., Galiero, R. and Bocchinfuso, G. Determination of total and polycyclic aromatic hydrocarbons in aviation jet fuel, *J. Chromatogr. A*, 2003, **985**, (1-2), pp 197–203. https://doi.org/10.1016/S0021-9673(02)01826-5

[24] ASTM Standard D1655-22a. Standard specification for aviation turbine fuels, *ASTM Int.,* 2022. https://doi.org/10.1520/D1655-22A

[25] Sadeghbeigi, R. Chapter 3 - FCC feed characterization, in R. Sadeghbeigi (Ed), *Fluid Catalytic Cracking Handbook*, 3rd ed, Butterworth-Heinemann, 2012, Oxford, pp 51–86. https://doi.org/10.1016/B978-0-12-386965-4.00003-3

[26] Yang, J., Xin, Z., He, Q., Corscadden, K. and Niu, H. An overview on performance characteristics of bio-jet fuels, *Fuel*, 2019, **237**, pp 916–936. https://doi.org/10.1016/j.fuel.2018.10.079

[27] Hamilton, J., Sadat, Y., Dwyer, M., Ghali, P. and Khandelwal, B. Thermal stability and impact of alternative fuels, in *Aviation Fuels*, Elsevier , 2021, pp 149–218. https://doi.org/10.1016/B978-0-12-818314-4.00003-0

[28] Chen, K. and Liu, H. The impacts of aromatic contents in aviation jet fuel on the volume swell of the aircraft fuel tank sealants, *SAE Int. J. Aerospace*, 2013, **6**, (1), p 350. https://doi.org/10.4271/2013-01-9001

[29] Bulzan, D., Tacina, K.M., Anderson, B., Beyersdorf, A., Wey, C., Howard, R., Winstead, E., Corporan, E., Dewitt, M.J., Klingshirn, C., Herndon, S., Miake-Lye, R., Timko, M., Wood, E., Liscinsky, D., Hagen, D., Lobo, P. and Phillip, W. Gaseous and particulate emissions results of the NASA alternative aviation fuel experiment (AAFEX), 2, 1195-1207-1207, 2010. doi: 10.1115/GT2010-23524

[30] Anuar, A., Undavalli, V., Khandelwal, B. and Blakey, S. Effect of fuels, aromatics and preparation methods on seal swell, *Aeronaut. J.*, 2021, **125**, (1291), pp 1542–1565. https://doi.org/10.1017/aer.2021.25

[31] Graham, J.L., Sa, R.C., Myers, K.J., Minus, D.K. and Harrison, W.E. Swelling of nitrile rubber by selected aromatics blended in a synthetic jet fuel, *Energy and Fuels*, 2006, **20**, (2), pp 759–765. https://doi.org/10.1021/ef050191x

[32] Zabarnick, S., Dewitt, M.J., Striebich, R.C., Gunasekera, T.S., Ervin, J.S., Briones, A.M., Shafer, L.M., Fernando, S.K., Graham, J.L. and West, Z.J. Fuels and Combustion Technologies for Aerospace Propulsion, 2016. Retrieved from https://apps.dtic.mil/sti/citations/AD1031932

[33] Graham, J., Rahmes, T., Ks, M., Belières, J., Kinder, J., Millett, S., Ray, J., Vannice, W. and Trela, J. Impact of alternative jet fuel and fuel blends on non-metallic materials used in commercial aircraft fuel systems, CLEEN

Project Final Report–Submitted by The Boeing Company, 10, 2011. Retrieved from https://www.faa.gov/sites/faa.gov/files/about/office_org/headquarters_offices/apl/Impact_of_Alternative_Jet_Fuel_and_Fuel_Blends.pdf

[34] Corporan, E., Edwards, T., Shafer, L., Dewitt, M.J., Klingshirn, C., Zabarnick, S., West, Z., Striebich, R., Graham, J. and Klein, J. Chemical, thermal stability, seal swell, and emissions studies of alternative jet fuels, *Energy Fuels*, 2011, **25**, (3), pp 955–966. https://doi.org/10.1021/ef101520v

[35] Adams, N.J., Baker, B.W., Vanbriesen, J.L., Durkin, D.P., Cowart, J.S., Schubbe, J.J. and Luning Prak, D.J. Additively manufactured O-rings: tensile strength and swelling behavior in the presence of gasoline and surrogate mixtures, *J. Mater. Eng. Perform.*, 2022, pp 1–13. https://doi.org/10.1007/s11665-022-07124-5

[36] Luning Prak, D.J., Adams, N.J., Vanbriesen, J.L., Cowart, J.S., Schubbe, J.S. and Baker, B.W. Swelling behavior and tensile strength of additively manufactured and commercial O-rings in the presence of linear, branched, cyclic, and aromatic compounds and alcohols, *J. Elastomers Plast.*, 2022, 00952443221104105. https://doi.org/10.1177/00952443221104105

[37] Graham, J., Rahmes, T., Kay, M., Belieres, J., Kinder, J., Millett, S., Ray, J. and Vannice, W. Alternative fuel, final report, FAA OTA DTFAWA-10-C-0030, 2011. Retrieved from https://www.faa.gov/sites/faa.gov/files/about/office_org/headquarters_offices/apl/Boeing_Alt_Fuels_Final.pdf

[38] Vangsness, M.D. and Vangsness, M.D. and Dayton Univ Research Institute. Best Practices for Fuel System Contamination Detection and Remediation, 2015. Retrieved from https://apps.dtic.mil/sti/pdfs/AD1031879.pdf

[39] ASTM standard D4306-20. Standard practice for aviation fuel sample containers for tests affected by trace contamination, *ASTM Int.*, 2020. https://doi.org/10.1520/D4306-20

[40] Arayapranee, W. Rubber abrasion resistance, *Abrasion Resist. Mater.*, 2012, **8**, pp 147–166. https://doi.org/10.5772/30556

[41] Chen, K. The compatibility study of aircraft fuel tank elastomers with synthesized paraffinic kerosine and its blends, *SAE Int. J. Aerospace*, 2014, **7**, pp 164–170. https://doi.org/10.4271/2014-01-9001.

[42] Faulhaber, C.J. Elastomer O-Ring Seal Swell Measurements for Sustainable Aviation Fuel Material Compatibility, 2022. Retrieved from https://ecommons.udayton.edu/uhp_theses/384